JOURNAL OF APPLIED ELECTROCHEMISTRY 7 (1977) 345–353

The anodic dissolution of lead in oxygenated and deoxygenated sulphuric acid solutions

R. D. ARMSTRONG, K. L. BLADEN

Electrochemistry Research Laboratories, School of Chemistry, The University, Newcastle-upon-Tyne, UK

Received 21 December 1976

Steady-state and impedance measurements were carried out in oxygenated and deoxygenated sulphuric acid solutions to investigate the effects of dissolved oxygen. Impedance measurements in deoxygenated sulphuric acid were used to determine values of C_0.

1. Introduction

Two useful reviews of the electrochemistry of lead [1, 2] have been compiled and a comprehensive list of papers is contained therein.

The kinetics of active dissolution and passivation of lead in H_2SO_4 have been investigated to a lesser extent [3–6] than the thermodynamics of the system which are relatively well understood [7, 8]. Hampson *et al.* [3] using fast linear sweep voltammetry on polycrystalline lead concluded that, in dilute H_2SO_4 and at lower sweep rates, the rate controlling mechanism for the anodic oxidation of Pb is the diffusion of SO_4^{2-} and HSO_4^- ions in solution. However, it seems more likely that Pb(II) species are responsible for the observed diffusion effects.

Archdale and Harrison [4, 5] showed that at low anodic potentials the oxidation of lead occurred by reversible dissolution to form Pb(II) species. At potentials above the critical value for the initiation of the solid-state reaction, direct anion attack occurs and a solid-state film is formed. Fleming *et al.* [6] concluded that in H_2SO_4 the species dissolving is a complex i.e. $PbSO_4$ or $PbHSO_4^+$ rather than Pb^{2+}.

Alternating current impedance techniques have been used to study the system [7, 10]. Lazarev *et al.* [7] studied the dependence of the capacitance and resistance of a lead electrode on the potential and found that the capacitance increased as the potential was made more anodic, reached a peak which they assign to Pb^{2+} ions passing from the surface into solution; and then dropped off sharply to 2–3 μF cm^{-2} when a passive film of $PbSO_4$ was formed. As a result of differential capacitance measurements in very dilute H_2SO_4 Carr *et al.* [9] showed that SO_4^{2-} anions are weakly adsorbed at the electrode. Strochkova *et al.* [10] carried out impedance measurements on smooth electropolished lead in H_2SO_4 solutions of various concentrations saturated with $PbSO_4$. They concluded that the equivalent circuit was correctly represented by the Warburg impedance and calculated values of $C_0\sqrt{D_0}$. By assuming a value for the diffusion coefficient ($D_0 = 10^{-5}$ cm^2 s^{-1}) they estimated values of the equilibrium concentration ($C_0 = 3 \times 10^{-5}$ mol l^{-1}) which approximates to the total solubility of lead species in the electrolyte thus indicating that the process is limited by diffusion of those species in the electrolyte which determine the potential.

Sato and Shiina [11] in polarization studies observed a second potential arrest which they assigned to the adsorption of oxygen on the electrode surface. Fleming *et al.* [6] concluded that dissolved oxygen has an effect both at negative potentials prior to dissolution and at more positive potentials when dissolution is the main process. Atkin *et al.* [12] generated oxygen at a rotating disc and measured the reduction current at a lead ring in 1, 2 and 5 M H_2SO_4 thus demonstrating that lead is capable of electrochemically reducing oxygen.

The present work was undertaken to investigate further the effects of dissolved oxygen in

sulphuric acid solutions as this is of importance, particularly with respect to the operation of sealed, maintenance-free lead acid batteries. Impedance measurements were carried out using new automated impedance equipment and the results analysed by digital computing techniques [13].

2. Experimental

Rotating disc electrodes of area 0·196 cm^2 were prepared from lead of purity 5 N (Koch-Light) embedded in a Teflon holder. Initially the lead electrodes were polished with successively finer grades of polishing alumina down to γ-alumina (particle size 1–5 μm) to produce a clean flat surface level with the surrounding Teflon. Immediately prior to experimentation the lead electrode was lightly etched in 0·75 M HNO_3 to produce a surface free of potential-determining oxides. It was then rinsed several times with triply distilled water and immersed in the working solution while still wet from the final rinse water. Once the rest potential had been determined the electrode was held at a cathodic potential close to the onset of hydrogen evolution, in solution deoxygenated for 16 h with BOC 'white-spot' nitrogen, to reduce and remove the etchant film and achieve a reproducible steady-state current value. In experiments using oxygenated solutions, oxygen was introduced into the cell at this stage and the current allowed to reach the limiting oxygen diffusion current value.

Measurements were carried out in a pyrex cell of conventional form with a bright platinum disc as a subsidiary electrode situated directly below and parallel to the working electrode. The reference electrode in a separate compartment was connected to the working solution 2 mm away from the working electrode via a Luggin capillary. Potentials are referred to the Hg/Hg_2SO_4 reference electrode in 3·0 M H_2SO_4 for work in H_2SO_4 solutions and to a hydrogen electrode in the same solution for work in $HClO_4$ solutions.

All solutions were made up using AristaR grade reagents with triply distilled water and deoxygenated for 16 h before use. Steady-state measurements were carried out using a potentiostat (Chemical Electronics, type TR70/2A) and the currents were traced out on a Y–t chart recorder (Chessel Flatbed).

Impedance measurements were obtained using an automated system based on the Solartron 1172 Frequency Response Analyser. This consists of a programmable generator to provide the perturbing sinusoidal signal, a correlator to analyse the systems response and a display to present the results. Using such equipment and various peripherals the results can be printed out, punched on tape and displayed graphically as a complex plane impedance plot using an X–Y recorder (Solartron 8700 A3).

Experiments were carried out at room temperature, 25 ± 2° C.

3. Results

3.1. *Steady-state currents*

The steady-state current–voltage curves for lead dissolution in H_2SO_4 are shown in Figs. 1(a) and (b) for both oxygenated and deoxygenated solutions. In the 3·0 M acid solution the height of the curve in oxygenated solution cannot be accounted for through the algebraic summation of the lead dissolution current and the diffusion-limited oxygen reduction current. In 0·1 M H_2SO_4 this discrepancy is much less pronounced. This suggests that some phenomenon associated with the anion concentration is responsible for the inhibition of the oxygen reduction reaction. Providing that the potential at which solid state formation of lead sulphate occurs is not reached the curves were all retraceable on return to more cathodic potentials.

In oxygenated H_2SO_4 solutions at potentials cathodic to − 1000 mV a limiting diffusion-controlled current due to oxygen reduction is observed. This shows that lead electrodes are capable of electrochemically reducing oxygen. Using these values of the limiting current and literature data for the solubility of oxygen [14] and the kinematic viscosity [15] the Levich equation

$$i_l = 0{\cdot}62nFACD^{2/3}\nu^{-1/6}\,\Omega^{1/2}$$

has been used to calculate the diffusion coefficient of oxygen in H_2SO_4 solution assuming that $n = 4$ i.e. that O_2 is reduced to water. It can safely be assumed that at a rotation speed of 53·3 Hz no supersaturation of solution with oxygen occurs. From Table 1 it can be seen that the value of the diffusion coefficient in 0·1 M

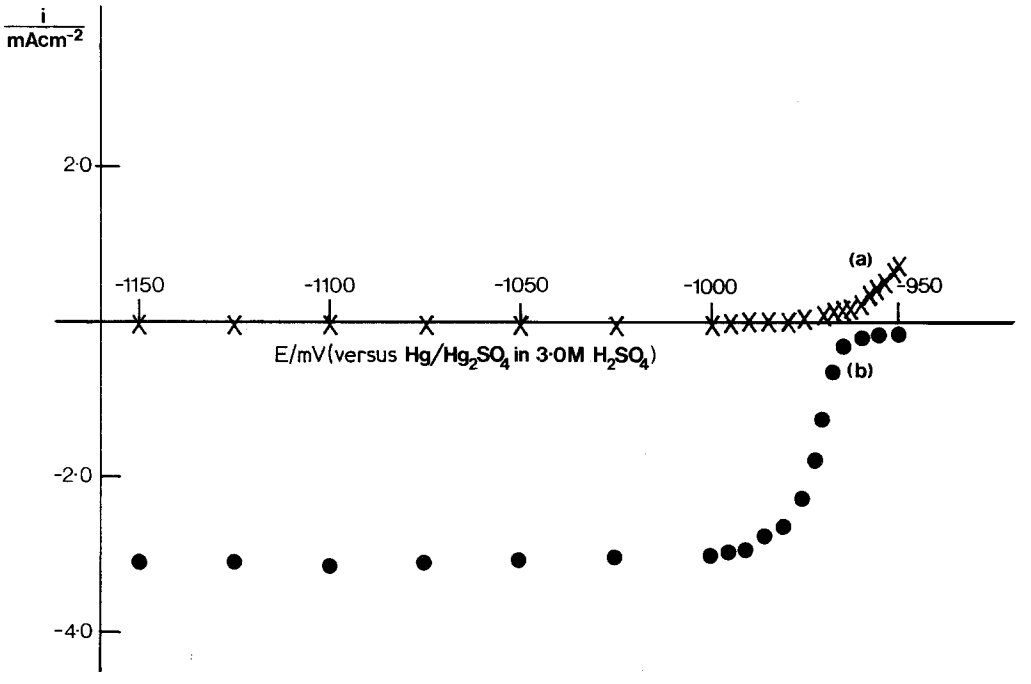

Fig. 1(a). Steady-state current–voltage curves for lead in 3·0 M H_2SO_4 at Ω 53·3 Hz. (X) deoxygenated (•) oxygenated solution.

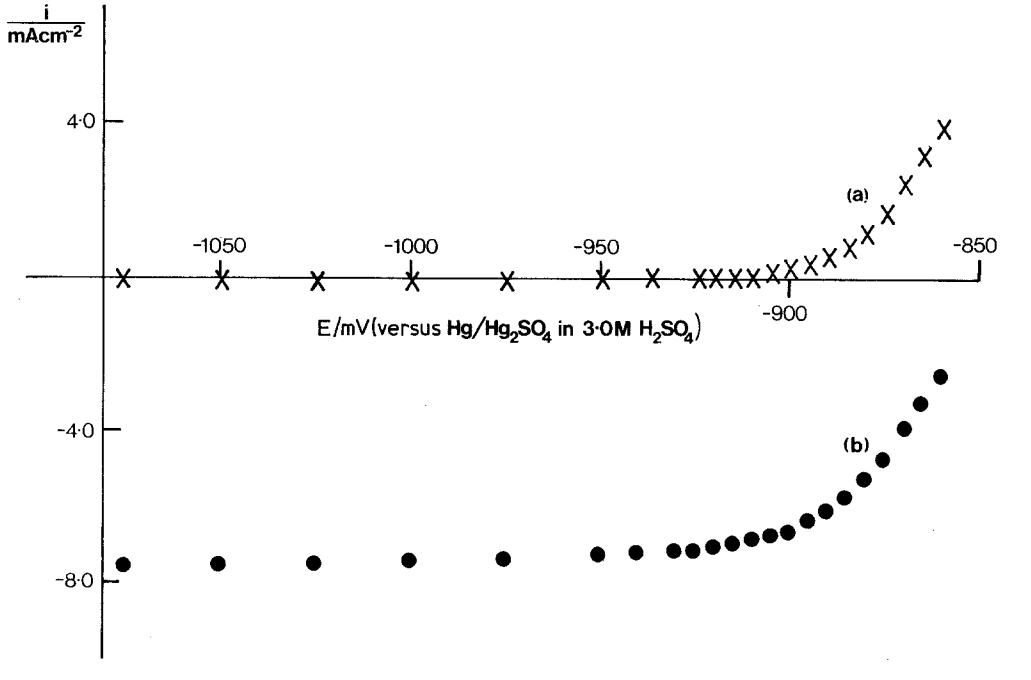

Fig. 1(b). Steady-state current–voltage curves for lead in 0·1 M H_2SO_4 at Ω = 53·3 Hz. (X) deoxygenated (•) oxygenated solution.

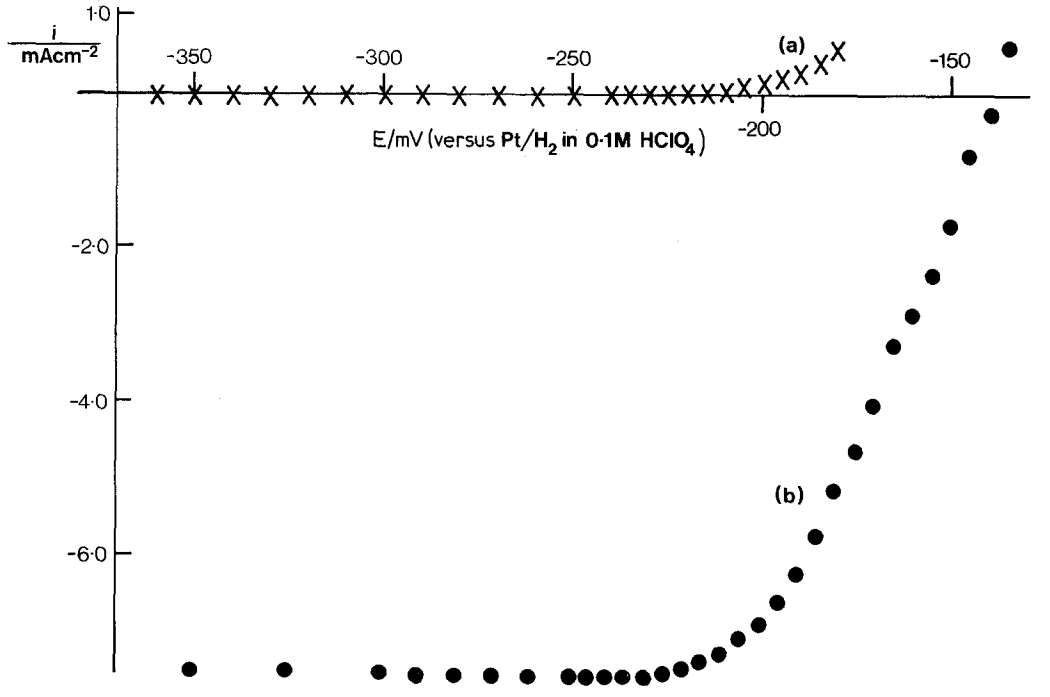

Fig. 1(c). Steady-state current–voltage curves for lead in 0·1 M $HClO_4$ at $\Omega = 53{\cdot}3$ Hz. (X) deoxygenated (•) oxygenated solution.

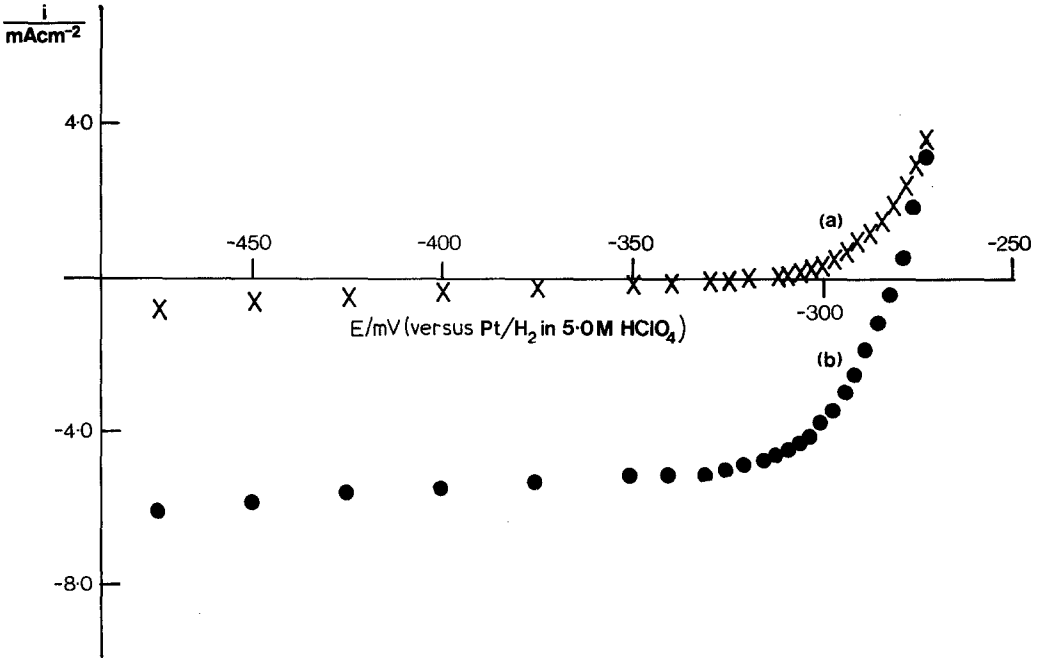

Fig. 1(d). Steady-state current–voltage curves for lead in 5·0 M $HClO_4$ at $\Omega = 53{\cdot}3$ Hz. (X) deoxygenated (•) oxygenated solution.

Table 1. Solubility and diffusion coefficients of oxygen in H_2SO_4

Concentration of sulphuric acid (mol dm^{-3})	*Wt. % of sulphuric acid* (g of solute/ 100 g of solvent)	*Kinematic viscosity*[42] *at 25° C* ($m^2 s^{-1}$)	*Solubility of oxygen*[43] *at 25° C and 1 atm pressure* (g mol dm^{-3})	*Limiting current at 25° C* (mA cm^{-2})	*Diffusion coefficient (from Levich Equation)* ($cm^2 s^{-1}$)	$D\eta/\eta_0$ ($cm^2 s^{-1}$)	η/η_0 *at 25° C*
0·1	1·00	$1·014 \times 10^{-6}$	$1·14 \times 10^{-3}$	7·436	$1·84 \times 10^{-5}$	$1·84 \times 10^{-5}$	0·9999
0·3	2·89	$1·037 \times 10^{-6}$	$1·06 \times 10^{-3}$	6·876	$1·831 \times 10^{-5}$	$1·90 \times 10^{-5}$	1·0377
3·0	25·00	$1·477 \times 10^{-6}$	$7·2 \times 10^{-4}$	3·102	$1·075 \times 10^{-5}$	$1·85 \times 10^{-5}$	1·720

H_2SO_4 is consistent with the diffusion coefficient of oxygen in water which has been previously reported as $1·90 \times 10^{-5}$ $cm^2 s^{-1}$ [14].

Similar behaviour is observed in deoxygenated and oxygenated perchloric acid solutions [Figs. 1(c), 1(d)]. In fact in 0·1 M $HClO_4$ the inhibition of the oxygen reduction reaction is more marked than in 0·1 M H_2SO_4. In 5 M $HClO_4$ the inhibition of oxygen reduction takes place even more strongly and eventually at − 260 mV against a hydrogen electrode in the same solution the two curves coincide [Fig. 1(d)]. Here again it seems that inhibition of oxygen reduction is concentration-dependent.

3.2. *Impedance measurements*

The impedance of the lead electrode in the dissolution region prior to film formation was investigated in 0·1, 0·3 and 3·0 M H_2SO_4 solutions. After a steady-state current had been attained at − 1200 mV (versus Hg/Hg_2SO_4 in 3·0 M H_2SO_4) an impedance spectrum was recorded. This shows a near vertical line which is in reality the high frequency part of a large semicircle indicating that the impedance is purely capactive. This plot allows the calculation of (C_{dl}) the double layer capacitance of the electrode and the solution resistance (R_{so}). The values of C_{dl} serve as a useful indication of the surface state of the electrode, values between 10–20 $\mu F\ cm^{-2}$ indicating a film-free surface. Values of C_{dl} were evaluated over the potential range of interest and are shown for the 3·0 M H_2SO_4 case in Fig. 2(a). It can be seen that there is a gradual increase in C_{dl} with potential up to the region of active dissolution where a sharp rise in C_{dl} is observed before it decreases again. The sharp increase in C_{dl} is probably due to anion adsorption prior to film formation which is evidenced by a decrease in C_{dl}. A similar effect is observed in 0·1 M $HClO_4$ (Fig. 2(b)) where in this case the perchlorate anion is the adsorbing species.

At potentials in the active dissolution region in 0·1 M H_2SO_4 the complex impedance plane plots showed a straight line of unity slope with almost no evidence of a charge transfer semicircle at high frequency. This straight line bent off at lower frequencies as the a.c. diffusion layer becomes comparable with the Nernst diffusion layer thus resulting in a deviation from the Warburg behaviour. The Warburg impedance is indicative of the diffusion of an oxidized species as a result of the dissolution process. The absence of a charge transfer semicircle is an indication that the dissolution process is both fast and reversible.

Analysis of the impedance in the active dissolution region was carried out by feeding the data in paper tape form into an IBM 370/167 computer with complex number facility. The experimental parameters, i.e. the real and imaginary parts of the impedance and the frequency of measurement, were treated in the following way. The solution resistance was subtracted from Z' and Z'' and they were then divided by the electrode area. The computer then selects points which lie on the 45° line rejecting scattered points and plots Z' and Z'' against $w^{-1/2}$. These plots are then used to produce the best straight line by a least squares analysis. The corresponding equations are

$$Z' = R_{ct} + \sigma w^{-1/2}$$

$$Z'' = \sigma w^{-1/2} + 2\sigma^2 C_{dl}$$

where σ is the Warburg coefficient. It was found that values of R_{ct} were too small to be measured.

Since the Warburg is the first shape in the impedance spectra it is also appropriate to carry out a R_p, C_p analysis of the data. The experimental data are therefore converted to the parallel components of resistance and capacitance. By a choice

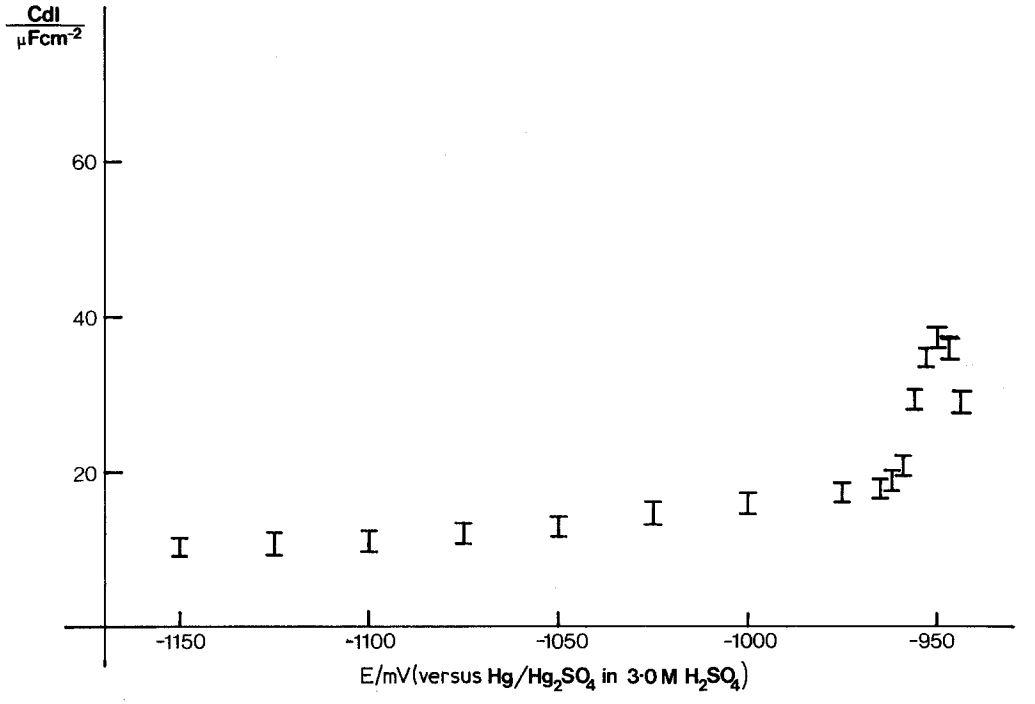

Fig. 2(a). Graph of C_{dl} against E in 3·0 M deoxygenated H_2SO_4.

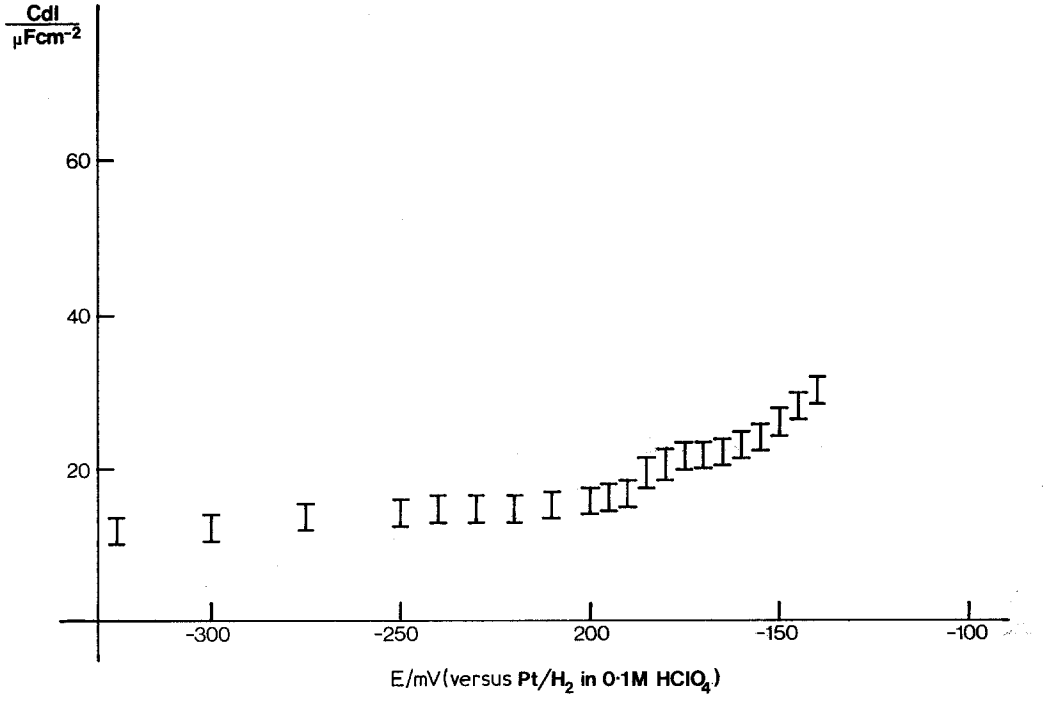

Fig. 2(b). Graph of C_{dl} against E in 0·1 M deoxygenated $HClO_4$.

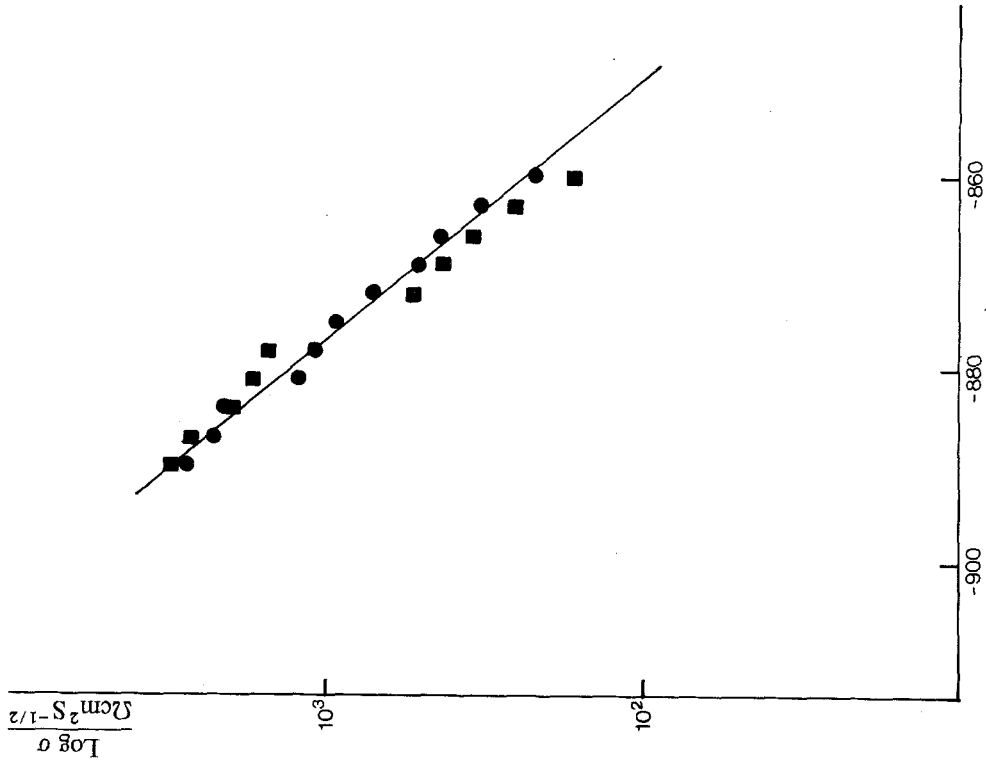

Fig. 3(b). Graph of log σ against E in 0·1 M H_2SO_4 in the active dissolution region. (•) From slope of Z' versus $w^{-1/2}$ plot; (■) from slope of Z'' versus $w^{-1/2}$ plot.

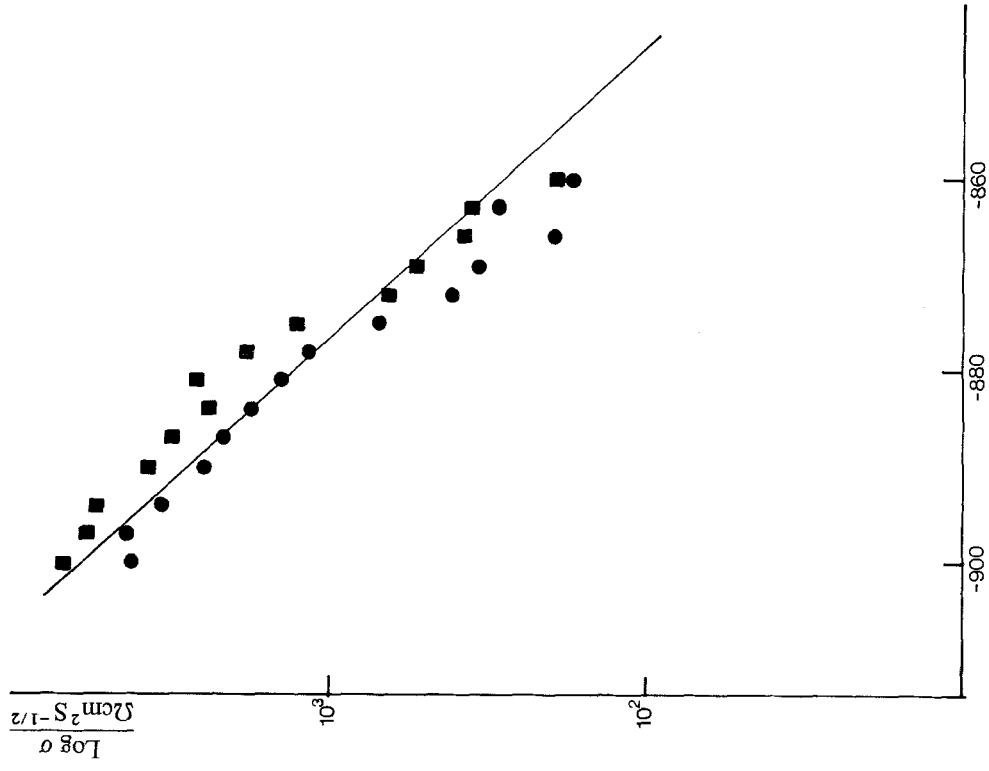

Fig. 3(a). Graph of log σ against E in 0·1 M H_2SO_4 in the active dissolution region. (•) From slope of R_p versus $w^{-1/2}$ plot; (■) from slope of C_p versus $w^{-1/2}$ plot.

Table 2. Comparison of calculated values of C_0 with literature values of the solubility of $PbSO_4$ in H_2SO_4 solutions

Concentration of H_2SO_4 (mol l^{-1})	*$Pb/PbSO_4$ Reversible potential* [mV (versus Hg/Hg_2SO_4 in 3·0 M H_2SO_4)]	*Estimated value of D_0 at 25° C* ($cm^2\ s^{-1}$)	*Value of C_0 from σ at 25° C* (mol l^{-1})	*Literature value of solubility of $PbSO_4$[16] at 25° C* (mol l^{-1})
0·1	−875	1×10^{-5}	$1{\cdot}57 \times 10^{-5}$	$1{\cdot}62 \times 10^{-5}$
0·3	−880	$9{\cdot}64 \times 10^{-6}$	$1{\cdot}75 \times 10^{-5}$	$1{\cdot}88 \times 10^{-5}$
3·0	−949	$5{\cdot}81 \times 10^{-6}$	$1{\cdot}32 \times 10^{-5}$	$1{\cdot}28 \times 10^{-5}$

of frequency limits the computer plots R_p and C_p against $w^{-1/2}$ where

$$R_p = 2\sigma/w^{1/2}$$

$$C_p = C_{dl} + w^{-1/2}/2\sigma.$$

It was found that the R_p versus $w^{-1/2}$ plots extrapolated to the origin as required for a reversible process. The C_p plots gave an intercept giving values of C_{dl} in agreement with those previously determined from $1/wC_s$. Hence four values of the Warburg coefficient were determined and are plotted as a function of potential in Figs. 3(a), 3(b). A mean slope of 30 ± 2 mV dec^{-1} was obtained from R_p, C_p values of σ and 27 ± 2 mV dec^{-1} from Z', Z'' plots. These values correspond to the expected 'Nernstian' slope of 30 mV dec^{-1} for a 2e reversible electron transfer. Thus the impedance measurements are consistent with the following dissolution reaction

$$Pb = Pb(II) + 2e.$$

At the $Pb/PbSO_4$ equilibrium potential the concentration of dissolving lead species was evaluated from the Warburg coefficient by the expression

$$C_0 = \frac{RT \times 10^3}{\sigma D_0^{1/2} 2^{1/2} n^2 F^2} \text{ mol } l^{-1}$$

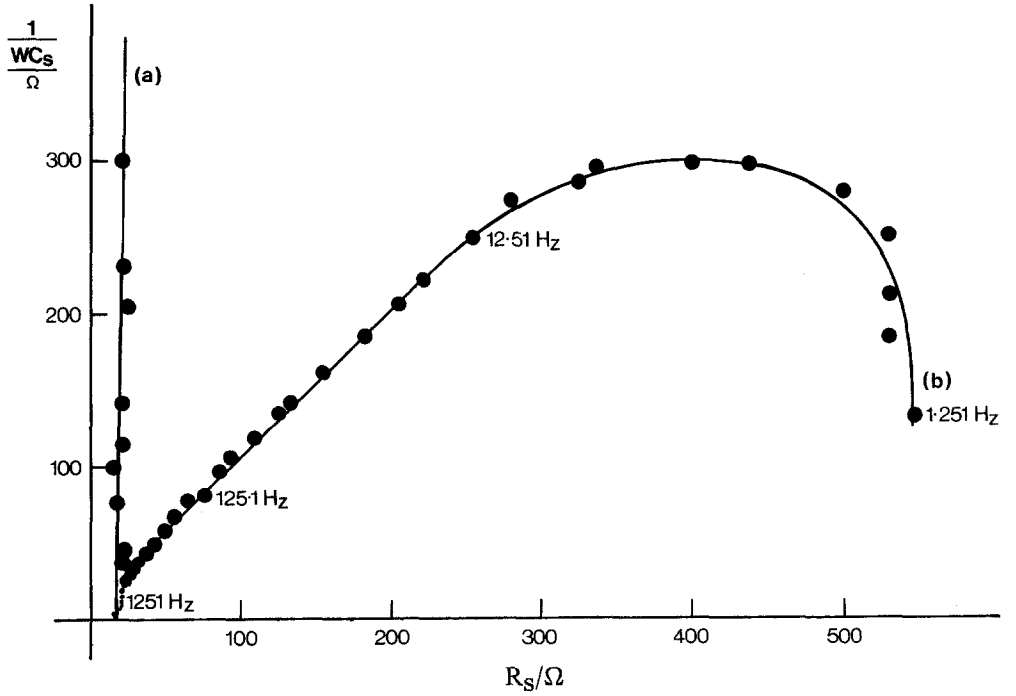

Fig. 4. Graph of R_S against $1/wC_S$ in 0·1 M H_2SO_4; (a) at −1200 mV; (b) at − 869 mV versus Hg/Hg_2SO_4. Frequency points in Hz, 10 points dec^{-1}.

assuming values for the diffusion coefficients. The results for 0·1, 0·3 and 3·0 M sulphuric acid are shown in Table 2 where a comparison is made with the solubility of $PbSO_4$ as determined by Craig and Vinal [16].

Fig. 4 shows a typical impedance spectrum (a) at − 1200 mV showing a near vertical line and (b) in the dissolution region. A few impedance spectra were recorded in oxygenated solutions and found to be quite different from those obtained for deoxygenated solutions.

4. Discussion

The results in oxygenated solution show that diffusion-controlled oxygen reduction occurs over a wide potential range. This is an important result as it opens up the possibility of a sealed maintenance-free battery operating in an oxygen recombination mode by using the lead negative electrode in a bifunctional role. However, in the lead dissolution region this reduction reaction appears to be inhibited by adsorption of anions. Experiments carried out in perchloric acid show that the perchlorate anion is capable of adsorption and having a similar inhibitory effect on oxygen reduction.

Impedance measurements show that the active dissolution of lead takes place by a fast reversible diffusion-controlled reaction to produce Pb(II) species which diffuse away from the electrode surface.

Acknowledgements

This work was based on a collaborative project with the Ever-Ready Company (G.B.) Limited, and we would like to thank Drs F. L. Tye and L. Baugh for helpful discussions.

References

[1] J. Burbank, A. C. Simon and E. Willihnganz, *Adv. Electrochem and Electrochem. Eng.* **8** (Ed. P. Delahay and C. W. Tobias) Interscience, New York (1971) p. 157.
[2] T. F. Sharpe, 'Encyclopaedia of the Electrochemistry of The Elements' (Ed. A. J. Bard) **1** Dekker, New York (1973) Chap. 5.
[3] J. P. Carr, N. A. Hampson and R. Taylor, *J. Electroanal. Chem.* **33** (1971) 109.
[4] G. Archdale and J. A. Harrison, *ibid* **34** (1972) 21.
[5] *Idem, ibid* **39** (1972) 357.
[6] A. N. Fleming, J. A. Harrison and J. Thompson, 'Power Sources 5' (Ed. D. H. Collins) Academic Press, London (1975) p. 1.
[7] V. F. Lazarev, V. I. Ovcharenko, A. J. Levin and V. M. Rudoi, *J. Appl. Chem. USSR* **38** (1965) 1284.
[8] T. F. Sharpe, *J. Electrochem. Soc.* **116** (1969) 1639.
[9] J. P. Carr, N. A. Hampson, S. N. Holley and R. Taylor, *J. Electroanal. Chem.* **32** (1971) 345.
[10] E. M. Strochkova. K. V. Rybalka and D. I. Leikis, *Elektrokhimiya* **11** (1975) 1439.
[11] E. Sato and T. Shiina, *J. Electrochem. Soc. Japan* **32** (1964) 148.
[12] J. Atkin, R. Bonnaterre and J. J. Laurent, *9th Int. Symp. Brighton* (1976).
[13] R. D. Armstrong, M. F. Bell and Adrienne A. Metcalfe, *J. Electroanal. Chem.* (in press).
[14] K. E. Gubbins and R. D. Walker, *J. Electrochem. Soc.* **112** (1965) 469.
[15] Handbook of Chemistry and Physics, (Ed. R. C. Weast) 53rd Ed. C.R.C. Press (1972-3) D-219.
[16] D. N. Craig and G. W. Vinal, *Nat. Bureau of Standards* **22** (1939) 55.